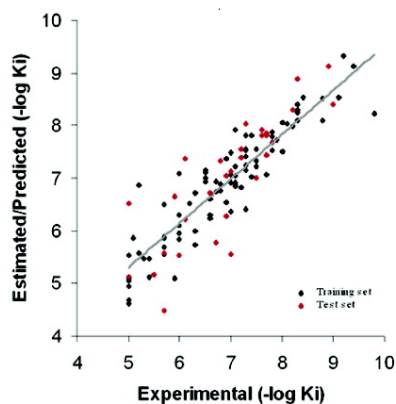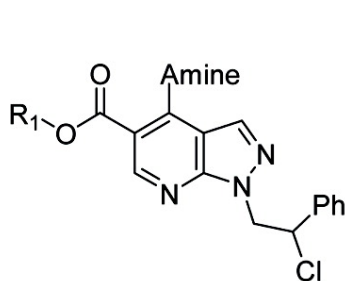Article

Synthesis and 3D QSAR of New Pyrazolo[3,4-*b*]pyridines: Potent and Selective Inhibitors of A Adenosine Receptors

Fabrizio Manetti, Silvia Schenone, Francesco Bondavalli, Chiara Brullo, Olga Bruno, Angelo Ranise, Luisa Mosti, Giulia Menozzi, Paola Fossa, Maria Letizia Trincavelli, Claudia Martini, Adriano Martinelli, Cristina Tintori, and Maurizio Botta

More About This Article

Additional resources and features associated with this article are available within the HTML version:

- Supporting Information
- Links to the 2 articles that cite this article, as of the time of this article download
- Access to high resolution figures
- Links to articles and content related to this article
- Copyright permission to reproduce figures and/or text from this article

View the Full Text HTML

Synthesis and 3D QSAR of New Pyrazolo[3,4-*b*]pyridines: Potent and Selective Inhibitors of A₁ Adenosine Receptors

Fabrizio Manetti,[†] Silvia Schenone,*,[‡] Francesco Bondavalli,[‡] Chiara Brullo,[‡] Olga Bruno,[‡] Angelo Ranise,[‡] Luisa Mosti,[‡] Giulia Menozzi,[‡] Paola Fossa,[‡] Maria Letizia Trincavelli,[§] Claudia Martini,[§] Adriano Martinelli,[||] Cristina Tintori,[†] and Maurizio Botta[†]

Dipartimento Farmaco Chimico Tecnologico, Università degli Studi di Siena, Via Aldo Moro, I-53100 Siena, Italy, Dipartimento di Scienze Farmaceutiche, Università degli Studi di Genova, Viale Benedetto XV n. 3, I-16132 Genova, Italy, Dipartimento di Psichiatria, Neurobiologia, Farmacologia e Biotecnologie, Università degli Studi di Pisa, Via Bonanno, I-56126, Italy, and Dipartimento di Scienze Farmaceutiche, Università di Pisa, Via Bonanno 6, I-56126, Pisa, Italy

A number of 4-aminopyrazolo[3,4-*b*]pyridines 5-carboxylic acid esters (**2**−**8**) were synthesized and evaluated for their binding affinity at the A₁, A₂ₐ, and A₃ adenosine receptors (AR), in bovine cortical membranes, as well as for their affinity toward human A₁AR (hA₁AR). Some of the new compounds were characterized by a high affinity and selectivity toward the A₁ receptor subtype, showing a significant improvement in comparison with other pyrazolo-pyridines previously reported in the literature. In particular the methyl ester **2h** as well as the isopropyl ester **5h**, both of them bearing a *p*-methoxyphenylethylamino side chain at the position 4, presented K_i values of 6 and 7 nM, respectively. To rationalize the relationships between structure and affinity of the novel compounds, a 3D QSAR model was also generated starting from compounds belonging to different classes of known A₁AR antagonists.

Introduction

Adenosine is an endogenous neuromodulator distributed in a wide variety of tissues, in both the periphery and the central nervous system.[1,2] This nucleoside exerts physiological response by interacting with four subtypes of receptors, named A₁, A₂ₐ, A₂ᵦ, and A₃,[3] belonging to the superfamily of G protein-coupled receptors.[4] The stimulation of adenosine receptors activates several effector systems, such as the enzyme adenylyl cyclase. Activation of A₁ and A₃AR leads to an inhibition of adenylyl cyclase activity, while activation of A₂ₐ and A₂ᵦAR causes a stimulation of adenylyl cyclase.[5] The four AR subtypes are also coupled with other second messenger systems, including calcium or potassium ion channels, phospholipase A₂ or C, and guanylate cyclase.[6] The physiological significance and functions of adenosine have been extensively studied. In the last two decades, a large number of adenosine receptor ligands (agonists and antagonists) have been developed.[5,7] Particularly, many efforts have been invested in the synthesis of A₁AR antagonists[8] that can stimulate cerebral activity by blocking the adenosine central inhibitory activity. A₁AR antagonists have therapeutic potential in the treatment of various form of dementia, such as the Alzheimer's disease,[5,9] depression,[10] and as cognition enhancers in geriatric therapy.[11] Moreover, A₁-AR antagonists are currently studied as potassium-saving diuretics and for the treatment of acute renal failure.[12] 4-Amino-substituted pyrazolo[3,4-*b*]pyridines,

as tracazolate, etazolate, and cartazolate, were originally identified as A₁AR antagonists,[13] during a wide screening on nitrogenated heterocyclic molecules related to purinic derivatives. Subsequently, a plethora of additional pyrazolo[3,4-*b*]pyridines has been also synthesized, among which the most active compound possess affinity of 0.3 μM for A₁AR, but scarce selectivity.[14] Finally, many other compounds with similar activity have been patented.[15]

In this context, we have recently synthesized a series of 4-amino-1-(2-chloro-2-phenylethyl)-1*H*-pyrazolo[3,4-*b*]pyridine-5-carboxylic acid ethyl ester derivatives **1** (Chart 1),[16,17] possessing an interesting antagonistic profile of affinity and selectivity toward A₁AR. Among them, the most active and selective compound (**1c**, Table 3), bearing a phenylethylamino side chain at the position 4, was characterized by a 50 nM affinity toward bovine A₁ receptors (bA₁AR), while showed only a 4 and 34% inhibition of the specific radioligand binding toward bA₂ₐ and bA₃AR, respectively.[16] Moreover, to get a better understanding of the structure−activity relationships (SAR) of the synthesized compounds and to find more active and A₁AR selective antagonists, we have also built a pseudoreceptor model[17] with the aim of guiding the design of new compounds by predicting their A₁AR affinity. Unfortunately, biological evaluation of several compounds suggested by the model did not give the expected results, demonstrating that the model itself was scarcely able to predict the activity of inhibitors subjected to modifications at the position 5.[18]

As a consequence, a new and more accurate model was required to better predict the activity of A₁AR inhibitors belonging to this family. To reach this goal, we have planned to synthesize compounds **2**−**8** (Table 1), bearing various substituents as the terminal portion
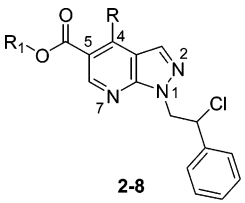
* To whom correspondence should be addressed. Tel: +39 010 3538866, fax: +39 010 3538358, e-mail: schensil@unige.it.
† Università degli Studi di Siena.
‡ Università degli Studi di Genova.
§ Dipartimento di Psichiatria, Neurobiologia, Farmacologia e Biotecnologie, Università degli Studi di Pisa.
|| Dipartimento di Scienze Farmaceutiche, Università di Pisa.

Table 1. Affinity of Compounds **2−8** toward A₁, A₂ₐ, and A₃ Adenosine Receptors

2-8

|			K_i (nM) or % inhibition[a]		
compd	R′	R	A₁[b]	A₂ₐ[c]	A₃[d]
2a	CH₃	NHcyclopropyl	251 ± 24	52%	n.d.
2b	CH₃	NHC₃H₇	170 ± 12	7671 ± 680	n.d.
2c	CH₃	1-pyrrolidinyl	4241 ± 402	0%	n.d.
2d	CH₃	4-morpholinyl	51%	0%	n.d.
2e	CH₃	NHCH₂C₆H₅	141 ± 12	7574 ± 632	n.d.
2f	CH₃	NHCH₂CH₂C₆H₅	88 ± 7	1232 ± 116	0%
2g	CH₃	NHCH₂CH₂C₆H₄-pCH₃	15 ± 2 (148 ± 18)	26%	40%
2h	CH₃	NHCH₂CH₂C₆H₄-pOCH₃	6 ± 1 (94 ± 7)	29%	41%
3a	C₂H₅	NHCH₂CH₂C₆H₄-pCH₃	22 ± 3	41%	38%
3b	C₂H₅	NHCH₂CH₂C₆H₄-pOCH₃	10 ± 1 (25 ± 4)	53%	49%
3c	C₂H₅	NHCH₂CH₂C₆H₄-oF	16 ± 1 (29 ± 3)	36%	53%
3d	C₂H₅	NHCH₂CH₂C₆H₄-mF	33 ± 3	25%	n.d.
3e	C₂H₅	NHCH₂CH₂C₆H₄-pF	12 ± 1 (16 ± 2)	30%	37%
3f	C₂H₅	NHCH₂CH₂C₆H₄-oCl	76 ± 3	0%	n.d.
3g	C₂H₅	NHCH₂CH₂C₆H₄-mCl	178 ± 11	21%	n.d.
3h	C₂H₅	NHCH₂CH₂C₆H₄-pCl	19 ± 1 (153 ± 13)	63%	46%
4a	C₃H₇	NHcyclopropyl	156 ± 15	1562 ± 123	2%
4b	C₃H₇	NHC₃H₇	145 ± 13	1388 ± 129	n.d.
4c	C₃H₇	1-pyrrolidinyl	2973 ± 265	1988 ± 176	n.d.
4d	C₃H₇	4-morpholinyl	2154 ± 201	31%	n.d.
4e	C₃H₇	NHCH₂C₆H₅	1374 ± 110	0%	n.d.
4f	C₃H₇	NHCH₂CH₂C₆H₅	130 ± 10	1358 ± 104	n.d.
5a	CH(CH₃)₂	NHcyclopropyl	36 ± 7	7503 ± 420	0%
5b	CH(CH₃)₂	NHC₃H₇	24 ± 4	11%	0%
5c	CH(CH₃)₂	1-pyrrolidinyl	1078 ± 90	30%	n.d.
5d	CH(CH₃)₂	4-morpholinyl	1822 ± 104	16%	n.d.
5e	CH(CH₃)₂	NHCH₂C₆H₅	559 ± 32	0%	n.d.
5f	CH(CH₃)₂	NHCH₂CH₂C₆H₅	31 ± 2	1517 ± 124	0%
5g	CH(CH₃)₂	NHCH₂CH₂C₆H₄-pCH₃	48 ± 3	26%	n.d.
5h	CH(CH₃)₂	NHCH₂CH₂C₆H₄-pOCH₃	7 ± 1 (17 ± 1)	34%	52%
5i	CH(CH₃)₂	NHCH₂CH₂C₆H₄-oCl	44 ± 3	13%	n.d.
5j	CH(CH₃)₂	NHCH₂CH₂C₆H₄-mCl	100 ± 7	14%	n.d.
5k	CH(CH₃)₂	NHCH₂CH₂C₆H₄-pCl	41 ± 2	27%	n.d.
6a	C₄H₉	NHcyclopropyl	895 ± 69	11%	0%
6b	C₄H₉	NHC₃H₇	959 ± 74	20%	n.d.
6c	C₄H₉	1-pyrrolidinyl	1893 ± 131	45%	n.d.
6d	C₄H₉	4-morpholinyl	63%	16%	n.d.
6e	C₄H₉	NHCH₂C₆H₅	27%	5%	n.d.
7a	CH(CH₃)C₂H₅	NHcyclopropyl	197 ± 12	33%	n.d.
7b	CH(CH₃)C₂H₅	NHC₃H₇	51 ± 5	40%	n.d.
7c	CH(CH₃)C₂H₅	NHCH₂CH₂C₆H₅	62 ± 4	46%	n.d.
8a	CH₂-cyclopropyl	NHC₃H₇	109 ± 7	23%	n.d.
8b	CH₂-cyclopropyl	NHCH₂C₆H₅	48 ± 4	54%	n.d.
8c	CH₂-cyclopropyl	NHCH₂CH₂C₆H₄-pCH₃	63 ± 5	4%	n.d.

[a] K_i values are means ± SEM of three separate assays, each performed in triplicate. [b] Displacement of specific [³H]DPCPX binding in bovine cortical membranes or percentage of inhibition of specific binding at 10 μM concentration. In parentheses, affinity values toward human A₁ CHO transfected cells are also reported. [c] Displacement of specific [³H]CGS21680 binding in bovine striatal membranes or percentage of inhibition of specific binding at 10 μM concentration. [d] Displacement of specific [¹²⁵I]AB-MECA binding in human A₃ CHO transfected cell membranes or percentage of inhibition of specific binding at 10 μM.

Chart 1

1
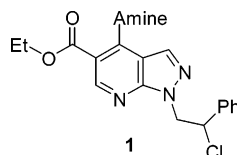
of the ester side chain. Variation of the ester function was envisaged as an interesting field of investigation to enlarge the knowledge on the SAR concerning such a substituent. Moreover, SAR data of our first generation A₁AR inhibitors (compounds **1**) evidenced the importance of either the 2-chloro-2-phenylethyl group at N1 or the cyclic and linear substituents at the position 4, for the activity toward A₁AR. Taking into account all these suggestions, we have chosen to keep the side chain at N1, while both the positions 4 and 5 were submitted to a variation of substituents. As a result, in the present study, we describe the synthesis and biological evaluation of a series of new 4-amino-(substituted)-1*H*-pyrazolo[3,4-*b*]pyridine-5-carboxylic acid esters (**2−8**), bearing the 2-chloro-2-phenylethyl chain at N1. The new compounds, along with their affinity data, were used to generate a highly predictive 3D QSAR model for antagonists of A₁AR.

Chemistry. The synthesis of the new compounds **2−8** is reported in Scheme 1. Acid hydrolysis (EtOH/H₂SO₄ at reflux for 24 h) of the 4-chloro-1-(2-chloro-2-phenyl-ethyl)-1*H*-pyrazolo[3,4-*b*]pyridine-5-carboxylic acid ethyl ester **9**, prepared in six steps from 2-hydrazino-1-phenylethanol and ethoxymethylene cyanoacetate according to our published procedure,[17] afforded the acid

Scheme 1[a]
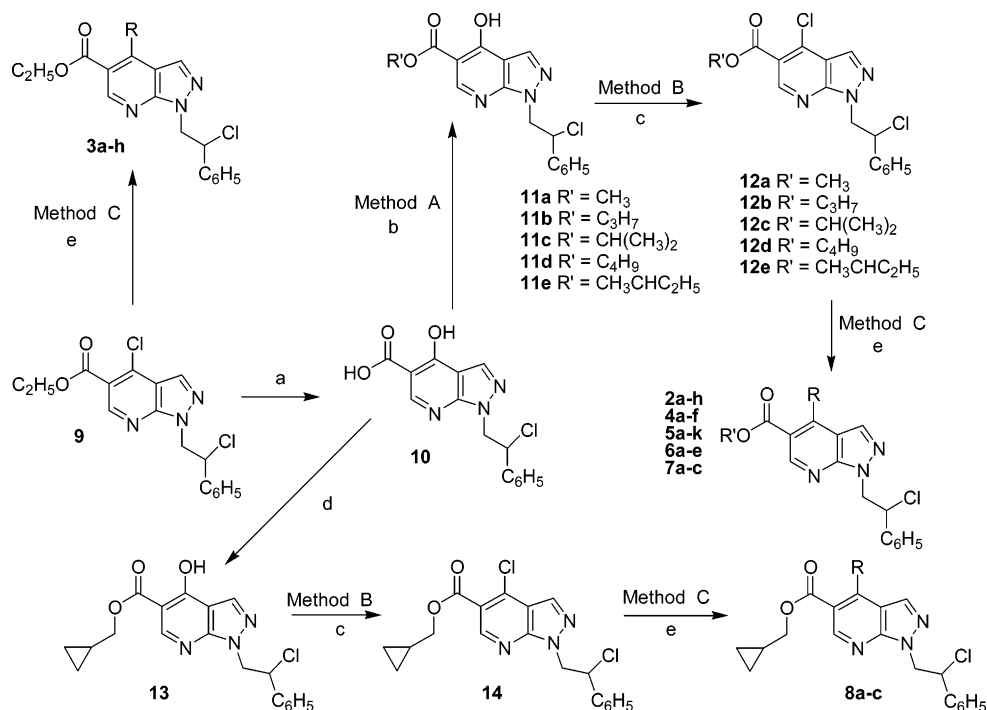
[a] Reagents: (a) 3 M H_2SO_4, EtOH, reflux, 24 h; (b) R'OH, concd H_2SO_4, 80 °C, 18 h; (c) $POCl_3$/DMF, $CHCl_3$, reflux, 8 h; (d) (1) $SOCl_2$, $CHCl_3$, reflux, 4 h, (2) cyclopropylmethanol, $CHCl_3$, reflux, 6 h; (e) amines, toluene, rt, 2 days.

10, where the chlorine atom at the position 4 was substituted by a hydroxy group. It is important to note that a basic hydrolysis caused an undesired dehydroalogenation at the N1 side chain, leading to the corresponding styryl derivative. The intermediate **10** was transformed in good yield into the corresponding ester derivatives **11a**−**e**, through a Fisher esterification with methyl, propyl, isopropyl, butyl, and *sec*-butyl alcohol, in the presence of concentrated H_2SO_4 (80 °C, 18 h) (Method A). On the other hand, the ester intermediate **13** was prepared by treating **10** with thionyl chloride at reflux, and then, without isolation of the intermediate acyl chloride, with cyclopropylmethanol in $CHCl_3$ at reflux for 6 h.

Treatment of **11a**−**e** and **13** with the Vilsmeier complex ($POCl_3$:DMF 1:1) in $CHCl_3$ at reflux for 8 h (Method B) afforded the corresponding 4-chloro derivatives **12a**−**e** and **14**, respectively, that were in turn purified by chromatography with Florisil and $CHCl_3$ as the eluant (55−70% yield). Regioselective substitution of the C4 chloride substituent of compounds **9**, **12** and **14** with an excess of various amines (Method C) led to the final compounds **2**−**8**, in a very satisfactory yield (65−90%).

Biology. Compounds were tested for their ability to displace [3H]-8-cyclopentyl-1,3-dipropylxanthine, [3H]D-PCPX, from A_1AR, and [3H]-2-[[4-(2-carboxyethyl)phenethyl]amino]-5-(*N*-ethylcarbamoyl)adenosine, [3H]CGS-1680, from $A_{2A}AR$. The ability of the most active compounds to displace [125I]-*N*-(3-iodo-4-aminobenzyl)-5-*N*-methylcarboxamidoadenosine, [125I]AB-MECA, from A_3-AR was also evaluated in CHO cells transfected with human A_3AR.[19] Moreover, the most A_1AR selective compounds were also tested for their affinity toward human A_1AR CHO transfected cells. Binding affinities toward A_1 (both bovine and human receptors), A_{2A}, and A_3AR,

Table 2. Intrinsic Activity of **2h** and **5h** toward A_1AR, Expressed as GTP Shift[a]

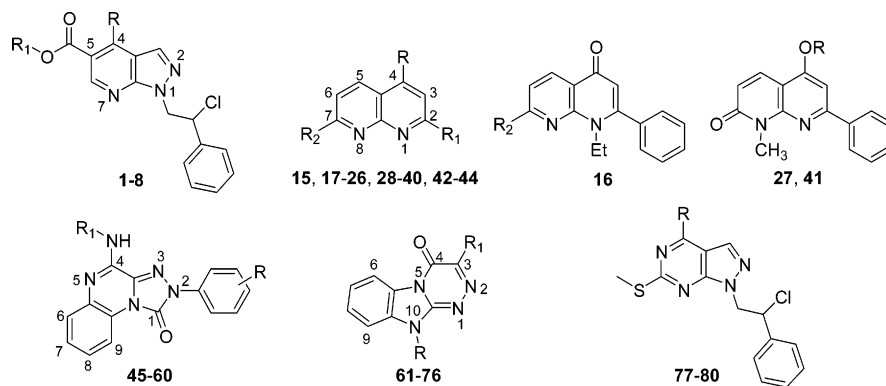| compd | K_i (A_1AR, nM) | | GTP shift |
	−GTP	+ GTP	
R-PIA	4.2 ± 0.3	20 ± 1	4.7
2h	6.3 ± 0.3	7.3 ± 0.4	1.1
5h	7.2 ± 0.5	7.7 ± 0.3	1.0

[a] Displacement of [3H]DPCPX from bovine cortical membranes in the absence and in the presence of 1 mM GTP. Values were taken as mean ± SEM from three different experiments.

expressed as affinity constant values (K_i) or % inhibition of specific radioligand binding, are reported in Table 1.

Moreover, selected compounds (namely, **2h** and **5h**) were also profiled in functional assays for their intrinsic activity at the A_1AR (displacement of [3H]DPCPX from bovine cortical membranes in the absence and in the presence of 1 mM GTP) and results are reported in Table 2. No significative GTP shift was evidenced, suggesting that they elicited an antagonist profile. In contrast, *R*-PIA, used as a standard agonist, exhibited a larger GTP shift value of 4.7.

SAR Analysis. The new pyrazolo-pyridines **2**−**8** reported in this paper showed a very interesting A_1AR affinity profile that, together with affinity data already reported for a series of pyrazolo-pyridine ethyl esters,[16] allowed better clarification of the role of the amino and the ester substituents at the position 4 and 5, respectively, in the modulation of the affinity toward A_1AR.

With the aim of investigating their influence in defining affinity toward adenosine receptors, various substituents (F, Cl, Me, OMe) have been introduced on the phenyl ring of the phenylethylamino moiety at the position 4 of the ethyl ester parent compound **1c** (Table 3), leading to derivatives **3** (Table 1). With the exception of compounds **3f** and **3g**, bearing an ortho and meta chloro substituent, respectively, and found to be less

Table 3. Structures, Experimental, and Estimated/Predicted Affinity of Compounds **1–8, 15–80** toward A₁AR

				A₁AR affinity ($-\log K_i$)[b]	
compd[a]	R	R₁	R₂	exp	calcd
1a	4-morpholinyl	C_2H_5		6.3	5.7
1b	$NHCH_2C_6H_5$	C_2H_5		6.9	6.5
1c	$NHCH_2CH_2C_6H_5$	C_2H_5		7.3	7.6
1d	NHC_3H_7	C_2H_5		7.0	7.5
1e[c]	NHcyclopropyl	C_2H_5		6.9	7.0
1f[c]	1-pyrrolidinyl	C_2H_5		7.0	5.6
2a	NHcyclopropyl	CH_3		6.6	6.6
2b	NHC_3H_7	CH_3		6.8	6.8
2c	1-pyrrolidinyl	CH_3		5.4	5.5
2d	4-morpholinyl	CH_3		5.0	5.5
2e[c]	$NHCH_2C_6H_5$	CH_3		6.9	6.3
2f	$NHCH_2CH_2C_6H_5$	CH_3		7.1	6.9
2g[c]	$NHCH_2CH_2C_6H_4-pCH_3$	CH_3		7.8	7.7
2h	$NHCH_2CH_2C_6H_4-pOCH_3$	CH_3		8.2	8.0
3a[c]	$NHCH_2CH_2C_6H_4-pCH_3$	C_2H_5		7.7	7.8
3b	$NHCH_2CH_2C_6H_4-pOCH_3$	C_2H_5		8.0	8.0
3c	$NHCH_2CH_2C_6H_4-oF$	C_2H_5		7.8	7.5
3d	$NHCH_2CH_2C_6H_4-mF$	C_2H_5		7.5	7.3
3e	$NHCH_2CH_2C_6H_4-pF$	C_2H_5		7.9	7.7
3f	$NHCH_2CH_2C_6H_4-oCl$	C_2H_5		7.1	7.0
3g	$NHCH_2CH_2C_6H_4-mCl$	C_2H_5		6.7	6.9
3h	$NHCH_2CH_2C_6H_4-pCl$	C_2H_5		7.7	7.8
4a	NHcyclopropyl	C_3H_7		6.8	6.9
4b[c]	NHC_3H_7	C_3H_7		6.8	7.3
4c[c]	1-pyrrolidinyl	C_3H_7		5.5	5.2
4d	4-morpholinyl	C_3H_7		5.7	5.6
4e[c]	$NHCH_2C_6H_5$	C_3H_7		5.9	6.7
4f	$NHCH_2CH_2C_6H_5$	C_3H_7		6.9	7.4
5a[c]	NHcyclopropyl	$CH(CH_3)_2$		7.5	7.0
5b	NHC_3H_7	$CH(CH_3)_2$		7.7	7.4
5c[c]	1-pyrrolidinyl	$CH(CH_3)_2$		6.0	5.5
5d	4-morpholinyl	$CH(CH_3)_2$		5.7	5.7
5e	$NHCH_2C_6H_5$	$CH(CH_3)_2$		6.2	6.5
5f	$NHCH_2CH_2C_6H_5$	$CH(CH_3)_2$		7.5	7.5
5g	$NHCH_2CH_2C_6H_4-pCH_3$	$CH(CH_3)_2$		7.3	7.8
5h	$NHCH_2CH_2C_6H_4-pOCH_3$	$CH(CH_3)_2$		8.1	8.0
5i	$NHCH_2CH_2C_6H_4-oCl$	$CH(CH_3)_2$		7.4	7.0
5j	$NHCH_2CH_2C_6H_4-mCl$	$CH(CH_3)_2$		7.0	6.9
5k	$NHCH_2CH_2C_6H_4-pCl$	$CH(CH_3)_2$		7.4	7.8
6a	NHcyclopropyl	C_4H_9		6.0	5.8
6b	NHC_3H_7	C_4H_9		6.0	6.1
6c[c]	1-pyrrolidinyl	C_4H_9		5.7	4.8
6d	4-morpholinyl	C_4H_9		5.0	4.7
6e	$NHCH_2C_6H_5$	C_4H_9		5.0	4.6
7a	NHcyclopropyl	$CH_3CHC_2H_5$		6.7	6.7
7b	NHC_3H_7	$CH_3CHC_2H_5$		7.3	7.4
7c[c]	$NHCH_2CH_2C_6H_5$	$CH_3CHC_2H_5$		7.2	7.6
8a	NHC_3H_7	CH_2-cyclopropyl		7.0	7.1
8b	$NHCH_2CH_2C_6H_5$	CH_2-cyclopropyl		7.3	7.2
8c[c]	$NHCH_2CH_2C_6H_4-pCH_3$	CH_2-cyclopropyl		7.2	7.4
15[d]	OH	Ph	CH_3	8.3	8.4
16			CH_3	6.3	6.0
17	Cl	Ph	CH_3	6.0	7.1
18	OCH_3	Ph	CH_3	5.2	6.8
19	NH_2	Ph	CH_3	7.8	7.8
20	NHcyclohexyl	Ph	CH_3	7.5	7.2
21[d]	OH	p-FPh	CH_3	8.3	8.1

Table 3. (Continued)

				A$_1$AR affinity ($-\log K_i$)[b]	
compd[a]	R	R$_1$	R$_2$	exp	calcd
22[d]	OH	Ph	Br	9.1	8.5
23[d]	OH	Ph	Cl	9.8	8.2
24[c,d]	OH	Ph	OPh	7.6	7.8
25[d]	OH	Ph	OEt	8.3	8.2
26[d]	OH	Ph	OCH$_3$	8.8	8.1
27	CH$_3$			5.9	5.1
28[c]	NHNH$_2$	Ph	CH$_3$	7.0	7.1
29[d]	OH	Ph	N(CH$_3$)$_2$	9.2	9.3
30[d]	OH	Ph	NHcyclohexyl	7.1	7.2
31	OEt	Ph	Br	7.3	7.2
32	OEt	Ph	OEt	6.5	6.9
33[c,d]	OH	p-NH$_2$Ph	CH$_3$	8.2	8.3
34[c,d]	OH	m-NH$_2$Ph	CH$_3$	7.6	7.9
35[d]	OH	CH$_2$Ph	CH$_3$	5.7	5.9
36[d]	OH	H	CH$_3$	5.1	5.9
37[d]	OH	CH$_3$	OH	5.0	4.9
38[d]	OH	CH$_3$	NH$_2$	5.0	5.0
39[d]	OH	CH$_2$CH$_2$CH$_3$	CH$_3$	7.3	6.4
40[c,d]	OH	CH$_2$CH$_2$CH$_3$	NH$_2$	6.7	5.8
41	H			5.3	5.5
42[d]	OH	Ph	NHCOCH$_3$	6.5	7.1
43[c]	OPh	Ph	CH$_3$	6.1	7.4
44[d]	OH	Ph	H	7.8	7.9
45	H	H		8.0	7.5
46	H	cyclohexyl		8.8	8.5
47	H	cyclopentyl		9.4	9.1
48	p-CH$_3$	H		7.7	7.0
49[c]	m-CH$_3$	H		7.7	7.4
50	m−F	H		7.5	7.5
51	m-CH$_3$	cyclohexyl		8.4	8.5
52[c]	m−F	cyclohexyl		8.3	8.9
53[c]	m-CH$_3$	cyclopentyl		8.9	9.1
54[c]	m−F	cyclopentyl		9.0	8.4
55	p-OCH$_3$	H		6.5	7.0
56		CH$_2$Ph		7.3	7.5
57		CH$_2$CH$_2$Ph		8.3	8.2
58	p-Cl	cyclohexyl		7.1	7.9
59	p-Cl	COPh		7.0	6.4
60[c]	p-Cl	CONHPh		7.3	8.0
61	H	Ph		7.1	6.9
62	CH$_3$	Ph		7.2	6.8
63[c]	Ph	Ph		7.7	7.8
64	H	fur-2-yl		6.6	6.2
65[c]	CH$_3$	p-Cl−Ph		5.0	6.5
66	CH$_3$	p-OCH$_3$		5.7	6.5
67[c]	CH$_3$	fur-2-yl		6.1	6.2
68	CH$_3$	thien-2-yl		7.1	6.9
69	Ph	fur-2-yl		6.5	7.1
70	CH$_2$Ph	fur-2-yl		6.0	6.3
71	H	CH$_3$		5.4	5.1
72[c]	CH$_3$	CH$_3$		5.0	5.1
73	CH$_2$Ph	CH$_2$Ph		6.6	6.3
74[c]	H	p-OH-Ph		6.6	6.7
75	H	m,p-OH		6.3	6.7
76	H	m,p-OCH$_3$		5.7	5.9
77	NHC$_3$H$_7$			6.0	5.9
78[c]	NHC$_4$H$_9$			5.7	5.6
79	NHcyclohexyl			5.2	5.6
80	NHCH$_2$CH$_2$Ph			5.0	5.1

[a] Compounds **1**, **15−44**, **45−60**, **61−76**, and **77−80** are taken from ref 16, 30, 31, 19, and 18, respectively. [b] Estimated values (expressed as $-\log K_i$) are for compounds belonging to the training set, predicted values are for compounds of the test set (expressed as $-\log K_i$). [c] Test set compounds. All the remaining molecules belong to the training set. [d] Such compounds were modeled in their quinoid form (i.e., with a quinoid oxygen atom at the position 4 and a protonated nitrogen at the position 1 of the cyclic core), according to ref 30.

active than the corresponding unsubstituted parent compound (76 and 178 nM, respectively, versus 50 nM), all the remaining compounds of this subclass showed improved activity (ranging from 10 to 33 nM). In detail, the best active compounds of this series (**3b** and **3e**) showed the para position substituted with a methoxy or a fluoride group, leading to an activity of 10 and 12 nM, respectively. Moreover, it is also important to note

that the fluoro substitution at the various positions on the phenyl ring was more profitable for affinity with respect to the corresponding chloro group (**3c** versus **3f**, **3d** versus **3g**, and **3e** versus **3h**).

Affinity values of compounds **2** were found comparable to those of both the corresponding ethyl analogues **3** and the derivatives previously published by our research group.[16] Moreover, **2h**, with a K_i value of 6 nM,

was the most active pyrazolo-pyridine derivative reported in this paper.

A further lengthening of the ester alkyl chain to a propyl and a butyl group led to compounds **4** and **6**, respectively, with affinity values in the micromolar range (spanning from 130 to 2973 nM), suggesting that the best linear alkyl group for the ester moiety was the ethyl or the methyl substituent. Very interestingly, when the alkyl ester was branched to an isopropyl group, such as in compounds **5**, good affinity values were found for particular substituents at the position 4 of the core structure. In particular, small aliphatic or cycloaliphatic groups such as the propylamino (**5b**) and cyclopropylamino (**5a**) moiety gave affinity of 24 and 36 nM, respectively, while larger and cyclic amines, such as 1-pyrrolidinyl (**5c**) and 4-morpholinyl (**5d**), were associated with very lower affinity (1078 and 1822 nM, respectively). Similarly, affinity for the benzylamino derivative **5e** was found in the low micromolar range (559 nM), while the phenylethylamino compound **5f** showed an affinity of 31 nM, comparable or better with respect to all the other phenylethylamino derivatives (compare with the affinity of **2f**, 88 nM; **1c**, 50 nM; **4f**, 130 nM; **7c**, 62 nM; and **8b**, 48 nM). Introduction of substituents on the phenyl ring of the phenylethylamino moiety led in general to similar (**5g**, **5i**, and **5k**) or decreased (**5j**) affinity, with the exception of compound **5h**, showing a very high affinity (7 nM), comparable with that of the corresponding methyl and ethyl ester derivatives **2h** and **3b**, respectively.

Finally, increasing the size of the isopropyl chain of compounds **5** to both a *sec*-butyl and a cyclopropylmethyl substituent (compounds **7** and **8**, respectively), a drop in affinity was observed.

In summary, the optimal combination of the amino substituent and the ester group at the positions 4 and 5, respectively, seems to be a *p*-methoxyphenylethyl-amino chain together with a short aliphatic group, such as a methyl, ethyl, and isopropyl moiety.

Compounds with higher affinity toward bA₁AR were also tested for their affinity toward hA₁AR. Affinity of **3b**, **3c**, **3e**, and **5h** was found to be comparable with that toward bA₁AR (25 vs 10, 29 vs 16, 16 vs 12, 17 vs 7 nM, respectively, Table 1). On the other hand, the remaining compounds tested showed affinity values toward the human receptor from 8-fold (**3h**) to about 10- (**2g**) and 16-fold (**2h**) lower than those found toward the bovine receptor (153 vs 19 nM, 148 vs 15, and 94 vs 6 nM, respectively).

The new compounds showed very low or no affinity toward both A₂ₐ and A₃AR (Table 1), thus leading to a high selectivity toward A₁AR. In fact, K_i values toward A₂ₐAR were in the micromolar range for a few compounds, while for the remaining derivatives, only low percentages of inhibition of specific CGS21680 binding at 10 μM concentration, were found. Similarly, all the compounds tested for their affinity toward A₃AR showed very low percentages of inhibition of specific AB-MECA binding at 10 μM concentration.

3D QSAR Studies

Dataset Selection. A set of 116 compounds was assembled grouping the new derivatives together with additional compounds previously reported by us,[20] as
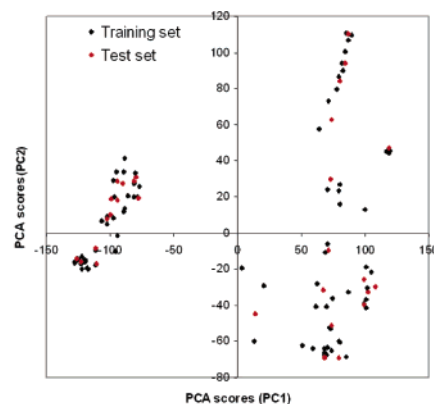

Figure 1. PCA score plot (*X*-axis and *Y*-axis report the first and the second components, respectively) for all 116 ligands. The uniform distribution of test set compounds (red dots) within clusters of training set compounds (black dots) suggests that selection between training set and test set was performed appropriately.

well as with molecules collected from the literature[21] (Table 3). It is important to note that within the huge amount of A₁AR inhibitors found in the literature, to ensure the highest homogeneity of biological data with respect to those of the new pyrazolo-pyridine derivatives, we have focused our attention on such compounds whose affinity toward A₁AR was obtained following the same experimental protocol applied for the new compounds. Moreover, derivatives found to be inactive (K_i > 10000 nM, Table 3) were also included in the original set of compounds, assigning them an arbitrary K_i value of 10000 nM, corresponding to a −log K_i = 5.0.[22]

Compounds of the original set were divided into a training set and a test set, according to the usual guidelines. In detail, either the training or the test set should contain compounds in such a way to maximize their structural diversity (that is, compounds belonging to the training set and to the test set should be representative of the molecular diversity of all the compounds under study) and uniformly span over the whole range of activity. As a result, the training set was constituted by 86 compounds, while an external validation set (test set) of 30 molecules was selected to test the predictive power of the model.

Moreover, with the purpose of checking the accuracy in the choice of training and test set compounds, following a protocol reported in the literature,[23] a PCA was performed by means of the program GOLPE,[24] using GRID interaction fields[25] as descriptors (corresponding to the interaction energies between appropriate chemical probes and all the compounds under study, see below). As a result, test set compounds (red dots, Figure 1) were uniformly distributed within clusters of training set compounds (black dots), suggesting that selection between training set and test set was performed appropriately.

Training set compounds are characterized by affinity values spanning about 5 orders of magnitude, the minimum value of 5.0 (expressed as −log K_i) being associated with compounds **37**, **38**, **80**, **2d**, **6d**, and **6e** and the maximum value of 9.8 being associated with compound **23**. Similarly, compounds belonging to the test set showed affinity value ranging from 5.0 (compounds **65** and **72**) to 9.0 (compound **54**), spanning over
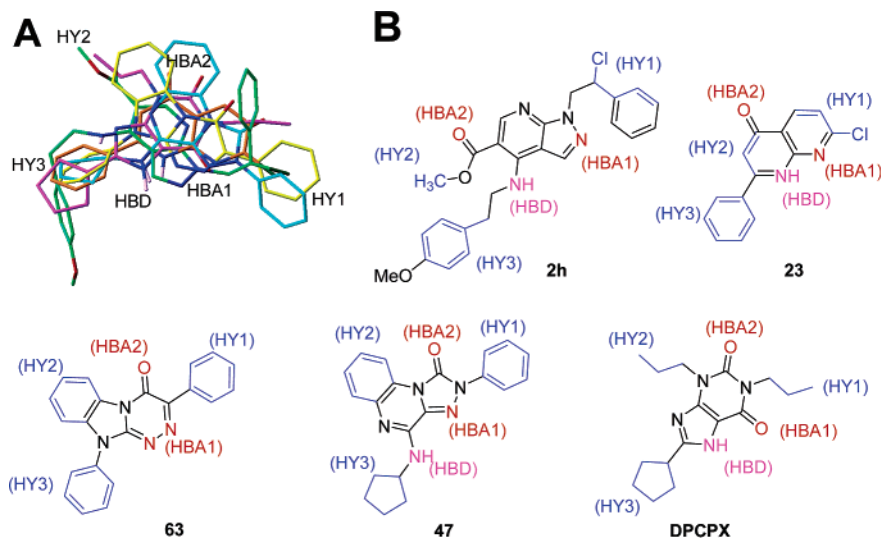
Figure 2. (A) Graphical representation of the alignment of compounds **2h** (green), **23** (orange), **63** (yellow), **47** (cyan), and DPCPX (purple), as obtained by application of the field fit alignment method of Cerius2. Pharmacophoric features are labeled, while heteroatoms and hydrogens bound to hydrogen bond donor groups are color coded following the atom-type notation. (B) A simplified view of the alignment where pharmacophoric elements have been labeled and color coded: hydrophobic regions, HY1-3, blue; hydrogen bond acceptor groups, HBA1-2, red; hydrogen bond donor groups, HBD, pink.

4 orders of magnitude. Training set compounds, along with their biological activity, were used to generate a 3D QSAR model for A_1AR antagonists.

In the first step, on the basis of the fact that the active conformation of the selected compounds is not known yet, we resorted to a molecular modeling approach to build the conformational populations to be used for the generation of the molecular alignment. A local minimum energy conformer of each compound was built using the 2D-3D sketcher implemented in the software Catalyst,[26] while the conformational space of all antagonists was then explored by a conformational search by means of the "best" procedure, keeping all conformations within 5 kcal/mol from the global minimum and specifying 250 as the maximum number of conformers.

Field Fit Alignment. It is well-known that one of the most important steps of a 3D QSAR study is represented by the alignment of the molecules under investigation. The alignment of all the molecules selected for this study was performed applying a protocol that combines the active analogue approach together with a field fit alignment method. The active analogue approach is usually used to search the bioactive conformers of the characteristic compounds of each family,[27] on the basis of the assumption that ligands able to bind the same site share the same three-dimensional arrangement of structural features essential for recognition to the receptor (the so-called pharmacophore pattern). The conformers found through this approach are in turn used as templates to fit the remaining molecules. For this purpose, the Align Molecules/Drug Discovery module in Cerius2[28] was used to perform the alignment of all the selected compounds. In detail, the low energy conformer of **23**, the most active compound among all the molecules under investigation, also characterized by a low conformational flexibility, was selected as the template structure. The alignment strategy was constituted by two steps. First, the most active compound of each chemical series, corresponding to **2h**, **47**, **63**, and **77**, was collected. All the conformers of each of the most active compounds was aligned to the target model

employing a rigid field fitting and using C (a generic carbon atom) as the probe. A fit similarity score was then calculated for all conformations and the conformer of each representative molecule that showed the higher fit was selected and used as the "active conformation" for its chemical family. In a second step, the active conformation of each structural class was used as the template structure to align all the remaining molecules of the same class. For these molecules, the conformer with the highest fit to the "active conformation" of the target model was selected and used in the next calculations. As a result, six common features were found (Figure 2), corresponding to three hydrophobic molecular portions (HY1-3), two hydrogen bond acceptors (HBA1-2), and a hydrogen bond donor group (HBD). In further detail, HY1 was filled by the chlorophenyl side chain of **2h**, the chloro substituent and part of the condensed pyridine ring of **23**, the phenyl ring at position 2 of **47**, and the phenyl ring at position 3 of **63**. Moreover, the methyl group of the ester function of **2h**, the C3 portion of **23**, and the fused benzene rings of both **63** and **47** were embedded into HY2. Finally, the aryl side chain at position 4 of **2h**, the phenyl ring at position 2 of **23**, the phenyl ring at position 10 of **63**, and the cyclopentyl ring of **47** were located within HY3. With the exception of **63**, the remaining three compounds showed a structural motif constituted by a hydrogen bond acceptor moiety (HBA1) close to a HBD. In particular, they were represented by N2 and the amino group of the C4 side chain of **2h**, N8 and N1(H) of **23**, and N3 and the amino group of the C4 side chain of **47**, respectively. Compound **63**, showing both N1 and N2 as possible hydrogen bond acceptors, lacked the HBD feature, thus accounting for its lowest binding affinity among the four compounds. The carbonyl group present on each of the four structures represented the remaining pharmacophoric feature HBA2.

The alignment proposed was in perfect agreement with a model of the bA_1AR recently proposed to rationalize SAR of a set of aryl-triazino-benzimidazoles.[19] In fact, HY1-3, HBA1-2, and HBD of the present model

corresponded to L2, L3, L1, HB2, HB3, HB1, respectively, of the model reported by Da Settimo and coworkers. Moreover, the alignment was also fully consistent with a previous pharmacophoric model built by us on the basis of a different collection of bA_1AR antagonists.[17]

Probe Selection. The ligands, aligned each other, were imported into the GRID software. Interaction energies between selected probes and each molecule were calculated using a grid spacing of 1 Å, while the size of the grid was set as large as to accommodate all the aligned ligands in all directions (along X, Y, and Z axes). Three probes were chosen to describe all the molecules. The C3 probe, corresponding to a methyl group, was used to account for steric contacts. The O probe (a sp^2 carbonylic oxygen) and the N2= probe (sp^2 amine $=NH_2^+$ cation) allowed to evaluate the ability of each compound to be a hydrogen bond donor and a hydrogen bond acceptor, respectively, as well as to calculate electrostatic potential fields on each ligand structure.

Variable Selection. Interaction energy values at each grid point were imported into the GOLPE program and used as independent variables to build a 3D QSAR model. However, it is well-known that many of the variables derived from the GRID analysis do not contribute to the correlation between chemical structure and biological activity, but they could be considered as noise, which decreases the quality of the model. As a consequence, to obtain a robust QSAR model, the no-significative variables were removed using the GOLPE program. From the 56376 active variables that were selected by GOLPE, an initial pretreatment performed by means of the advanced pretreatment tool (absolute values lower than 0.02 kcal/mol were set to zero and variables that exhibited only two values were removed) reduced the number of variables to 32690. Moreover, the D optimal preselection procedure was applied to obtain the most informative variables correlated with the biological activity. This procedure was repeated two times, using 50% as the reduction level and five components. Each selection of variables was preceded by calculation of a PLS model, on the basis of only the last selected variables. After D optimal variable preselection, the number of variables was further reduced to 8164.

A Smart Region Definition (SRD) algorithm was applied with the aim of selecting and grouping the regions of variables of highest importance for the model. The groups were then used in the Fractional Factorial Design (FFD) procedure replacing the original variables. FFD selection was applied three times, until no further improvement in the q^2 value was observed. As a result, the model obtained from the reduced set of variables (1247) was characterized by a significant enhancement of the predictive power, with respect to the parent model generated on the whole set of variables. In fact, the validation procedure (a cross-validation routine with five random sets of compounds) showed an improved internal predictive ability ($q^2 = 0.70$) for the final model with five components, in comparison to the model based on all the variables ($q^2 = 0.43$). This result allowed us to
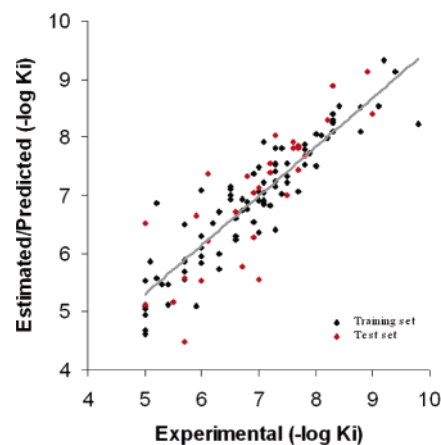

Figure 3. Experimental activity versus estimated/predicted activity in the final 3D QSAR model.

conclude that many of the original variables generated noise, instead of contributing to the robustness of the model.

Moreover, the predictive power of the model was further assessed by calculating affinity values for the test set compounds. As a result, a good correlation was found (0.63 as standard deviation of error of predictions, SDEP) between experimental and predicted affinity values of the external set of compounds (Figure 3 and Table 3).[29]

Interpretation of Contour Maps. One important feature of 3D QSAR analysis is the graphical representation of the model, usually aimed at making its interpretation easier. GOLPE provides several options to display the final model. Among these, PLS pseudo-coefficients are very useful because they allow the visualization of favorable and unfavorable interactions between the probes and the molecules under study. For this reason, GRID plots of PLS coefficients were analyzed by means of GOLPE with the purpose of getting a better understanding of the structure–activity relationships.

C3 Contour Map. Contour maps for the C3 probe indicated sterically unfavored and favored regions of space (cyan and yellow, respectively, Figure 4). In particular, regions with higher positive values (A, B, and C, Figure 4, yellow) corresponded to a profitable interaction between a molecular substituent and the methyl probe, contributing to ameliorate the affinity. On the contrary, the principal regions with negative values (D, E, F, G, and H, Figure 4, cyan) corresponded to an unfavorable interaction between a substituent of the molecule and the methyl probe, contributing to decrease the affinity. Figure 4a shows compound **2h** (characterized by the best K_i value, 6 nM) embedded into the contour map obtained with the C3 probe. The *p*-methoxyphenylethylamino group at the position 4, as well as the methyl group of the ester at the position 5, and the chloro substituent on the side chain at the position 1, being closed to the yellow regions of the map (C, B, and A, respectively), are suggested to have a steric contribution very profitable for affinity toward A_1AR. On the contrary, cyan volumes represented sterically not permitted regions. In fact, cyclic amino substituents such as pyrrolidino and morpholino moieties, or shorter side chains such as the benzyl group of compounds **2–8** showed steric hindrance, interacting with the region E
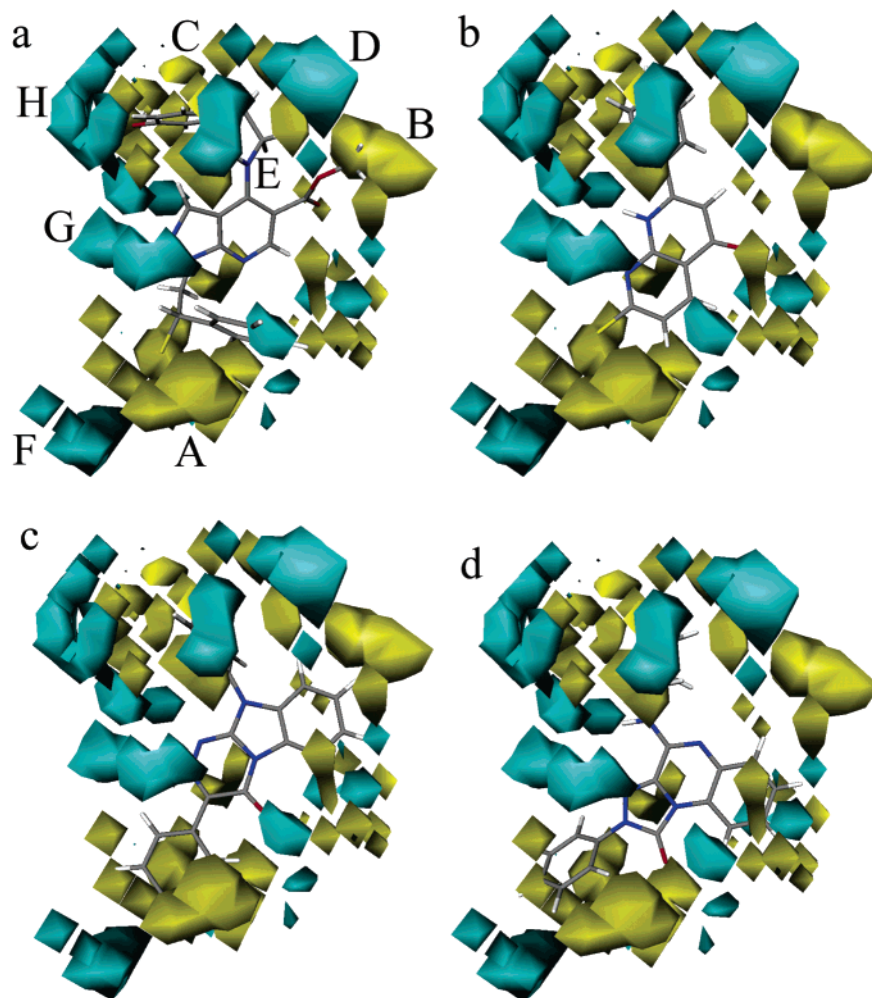
Figure 4. PLS coefficient plot obtained with the C3 probe. Compounds **2h** (a), **23** (b), **63** (c), and **47** (d) are embedded into positive (yellow) and negative (cyan) regions. Favorable interactions (i.e., an increase of $-\log K_i$) between a substituent and the probe occur in regions with positive coefficients (0.0003 kcal/mol level, positive regions, yellow), while unfavorable interactions (i.e., a decrease of $-\log K_i$) between a substituent and the probe occur in regions with negative coefficients (-0.0010 kcal/mol level, negative regions, cyan).

of the model. Region G shows that a substitution at the position 2 of the pyrazolo-pyridine nucleus is not permitted, while region H indicates that a substitution at the meta position of the phenylethyl side chain should result in a lack of affinity. The D region suggests that bulky substituents on the ester group, as butyl and *sec*-butyl chains could give a bad steric interaction. Figure 4b shows **23** characterized by favorable steric interactions with both regions A and C. Compound **63** (Figure 4c) has good contacts with regions A, B, and C, while **47** shows profitable steric contacts with regions A and C (Figure 4d).

N2= Contour Maps. Coefficient plots generated with the N2= probe mimic the hydrogen bond donor interactions. It is interesting to note that some positive and negative maps are positioned in the same portion of space also found for the C3 probe, indicating that the major effect of the N2= probe in these regions could be considered as of steric nature. In other words, in such regions, contribution of the N2= probe to the hydrogen bond contacts is low. Compound **2h** shows profitable interactions (region A and C, Figure 5a) involving both the ester group at the position 5 and the N2 atom as hydrogen bond acceptor moieties. This result, combined with that found for the C3 probe, clearly shows that the

ester function of the new pyrazolo-pyridine derivatives is a crucial structural element in defining affinity of such compounds toward A_1-AR. Compound **23** (Figure 5b) interacted favorably through its carbonyl moiety with both regions A and B, while the N8 contacted region C of the N2= map. Moreover, the carbonyl group at the position 4 of **63** is involved in a profitable interaction with the region B, while both N1 and N2 make hydrogen bond contacts with the region C of the N2= map (Figure 5c). In a similar way, Figure 5d shows good interactions between N3 of **47** and the region C of the map, while the carbonyl group and N5 have only a weak interaction with regions B and A, respectively.

O Contour Map. The contribution of the O probe to the PLS model represents both the ability to accept hydrogen bond contacts and make steric interactions. In fact, similarly to that found for the N2= probe, some portions of the O probe maps occupy similar regions of space previously identified with the C3 probe, suggesting that also the O probe is involved in steric contacts. Moreover, two regions (A and B, Figure 6) show profitable interactions with the hydrogen bond donor moieties of the molecules under investigation. In detail, the region A makes favorable interactions with the amino group at the position 4 of both **2h** and **47** (Figure 6a
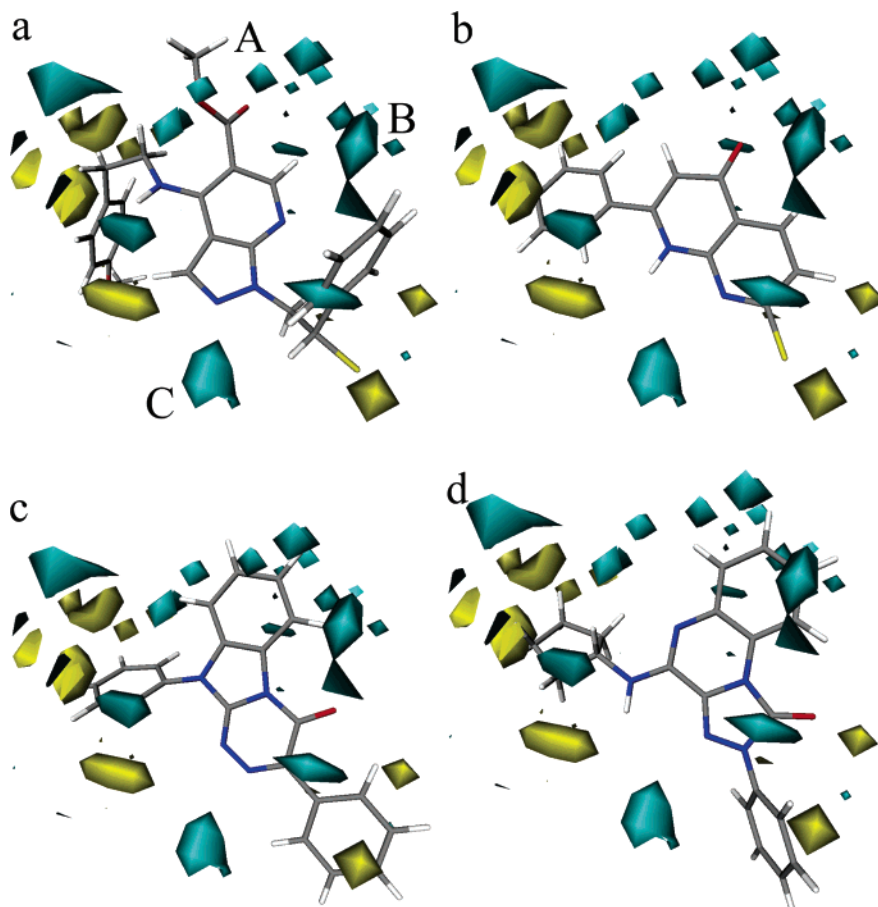
Figure 5. PLS coefficient plot obtained with the N2= probe. Compounds **2h** (a), **23** (b), **63** (c), and **47** (d) are embedded into positive (cyan) and negative (yellow) regions. Favorable interactions (i.e., an increase of $-\log K_i$) between a substituent and the probe occur in regions with negative coefficients (-0.0056 kcal/mol level, positive regions, cyan), while unfavorable interactions (i.e., a decrease of $-\log K_i$) between a substituent and the probe occur in regions with positive coefficients (0.0042 kcal/mol level, negative regions, yellow).

and 6d, respectively) while the region B interacts with the NH moiety of **23** (Figure 6b). No contact was found for compound **63** (Figure 6c), suggesting that the lower affinity of such a compound toward A₁AR in comparison to the affinity of **2h**, **23**, and **47**, could derive from the lack of hydrogen bond donor groups in its structure. As a consequence, the electrostatic component of the binding energy due to hydrogen bond donor groups in the inhibitor structure appears to be an important key in determining affinity toward A₁AR.

To verify such a hypothesis, starting from data derived from molecular structures (variables), we have evaluated how each probe was involved in defining the interactions with the studied compounds. Results highlighted that interactions with all the three probes (C3, N2=, O) contributed in the same measure to the activity (33.9%, 32.8%, 33.3%, respectively), suggesting that hydrogen bond acceptor groups, hydrogen bond donor groups and steric interactions were equally important in defining the affinity of all inhibitors toward the receptor.

In summary, results from calculations showed that the 3D QSAR model was able to explain, at the quantitative level, the structure−activity relationships of the 4-amino-1*H*-pyrazolo[3,4-*b*]pyridine-5-carboxylic acid esters. Substituents on the nitrogen at the position 4 and on the ester group at the position 5 were very important for affinity toward A₁AR. In particular, for

the ester group, a butyl or propyl chain seemed to be too bulky, giving unfavorable steric interactions, as showed by the methyl contour map. Differently, methyl, ethyl and isopropyl groups showed favorable steric interactions and resulted to be optimal substituents for this position.

Moreover, the structure of a phenylethylamino side chain at the position 4 was worthy of further consideration. In fact, while the linear portion of the chain (corresponding to the ethylamino spacer) was embedded, without any contact, into a narrow tunnel delimited by regions D and E of the C3 map (Figure 4), the phenyl ring was able to have profitable interactions with the region C. As a result of such interactions, a very interesting affinity was found for the phenylethyl derivatives with respect to compounds with shorter (benzyl) or bulkier (five or six membered heterocyclic rings) substituents at C4. This finding suggested that substituents at the position 4 should be characterized by a small volume close to the C4, while the distal portion of the side chain interacting with the region C of the C3 map tolerated larger groups. Accordingly, cyclic amino substituents such as pyrrolidino and morpholino moieties, or shorter side chains such as the benzyl group showed steric hindrance, interacting with the regions D and E of the model (Figure 4). In addition, the model showed that para substituted phenylethylamino side chains were preferred to the corresponding
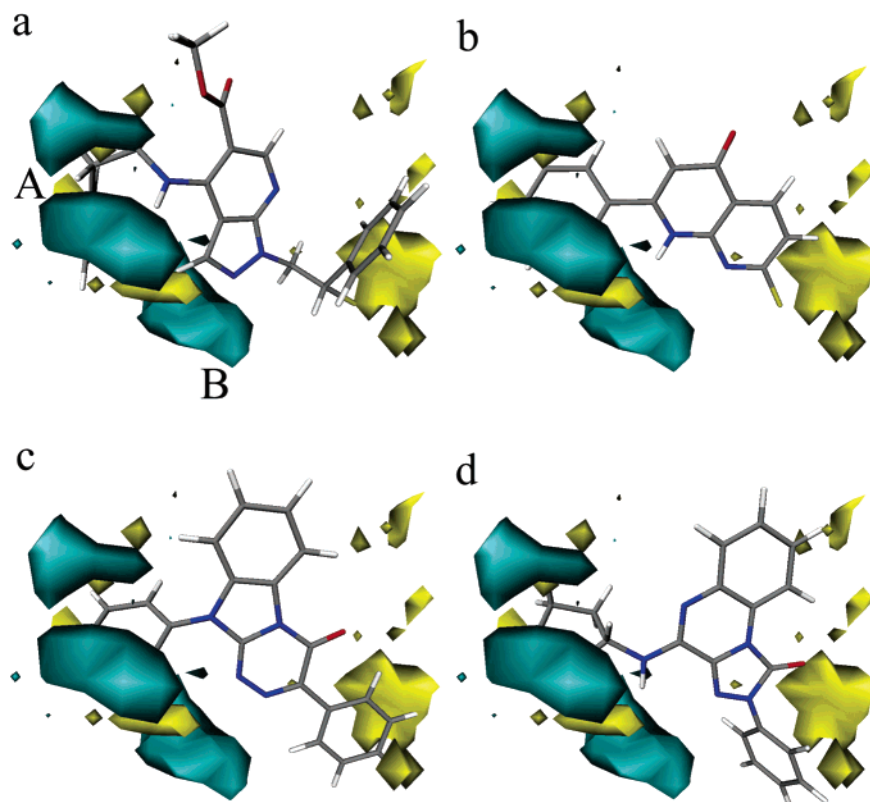
Figure 6. PLS coefficient plot obtained with the O probe. Compounds **2h** (a), **23** (b), **63** (c), and **47** (d) are embedded into positive (cyan) and negative (yellow) regions. Favorable interactions (i.e., an increase of $-\log K_i$) between a substituent and the probe occur in regions with negative coefficients (-0.0045 kcal/mol level, positive regions, cyan), while unfavorable interactions (i.e., a decrease of $-\log K_i$) between a substituent and the probe occur in regions with positive coefficients (0.0036 kcal/mol level, negative regions, yellow).

ortho and meta analogues (compare **3e** versus **3c** and **3d**; **3h** versus **3f** and **3g**; **5k** versus **5i** and **5j**).

It was also interesting to note that the 3D QSAR model was able to explain the low activity observed for 4-amino substituted 1-(2-chloro-2-phenylethyl)-6-methylthio-1*H*-pyrazolo[3,4-*d*]pyrimidines previously reported by us,[18] due to lack of any profitable hydrogen bond interaction with the region A of the N2= map.

Although the good predictivity for the biological activity of the test set compounds indicated the quality of the 3D QSAR study, however, we are confident that a model derived from affinity data toward bA$_1$AR cannot be considered as a reliable model also for affinity data toward the hA$_1$AR. In fact, it is well know that bA$_1$AR and hA$_1$AR are characterized by different antagonist binding sites,[30] reflecting differences in the activity data found for the same antagonists toward bA$_1$AR and hA$_1$-AR. As an example, compounds **2g**, **2h**, and **3h** showed affinity toward bA$_1$AR significantly different from affinity values toward hA$_1$AR.

Conclusions

Results reported in this paper strongly indicated that some of the newly synthesized pyrazolo-pyridines were good A$_1$AR ligands toward both human and bovine receptors, with high selectivity with respect to other adenosine receptors. In particular the methyl ester **2h** as well as the isopropyl ester **5h**, both of them bearing a *p*-methoxyphenylethylamino side chain at the position 4, possessed an affinity toward A$_1$AR about 8-fold and 7-fold higher than that of the corresponding parent

compound **1c**. In addition, several derivatives described in this paper revealed a higher affinity compared to the ethyl esters previously reported by us.[16] Moreover, selected compounds also showed affinity values in the nanomolar range toward hA$_1$AR. All the most interesting compounds were very selective for the A$_1$AR, showing low or no affinity toward both A$_2$AR and A$_3$AR.

From these experimental data, it was also evident that either substituents at the position 4 or the ester group at the position 5 played a very important role in defining the affinity properties of the studied compounds.

Finally, the new 3D QSAR model, built also using compounds **2−8**, demonstrated to have the knowledge for estimating/predicting the affinity of a very large number of inhibitors bearing to different structural classes. Such a model showed a better prediction ability with respect to the pseudoreceptor model previously published by us[17] and will be in turn used to provide suggestions to further optimize the new pyrazolo-pyridine derivatives.

Experimental Section

Chemistry. Starting materials were purchased from Aldrich-Italia (Milan, Italy). Melting points were determined with a Büchi 530 apparatus and are uncorrected. IR spectra were measured in KBr with a Perkin-Elmer 398 spectrophotometer. ^{1}H NMR spectra were recorded in a (CD$_3$)$_2$SO solution on a Varian Gemini 200 (200 MHz) instrument. Chemical shifts are reported as δ (ppm) relative to TMS as internal standard, *J* are expressed in Hz. [1]H patterns are described using the following abbreviations: s = singlet, d = doublet, dd = double

doublet, t = triplet, q = quartet, sx = sextet, sept = septet, m = multiplet, br = broad. All compounds were tested for purity by TLC (Merk, Silica gel 60 F$_{254}$, CHCl$_3$ as the eluant). Analyses for C, H, N were within ±0.3% of the theoretical value.

1-(2-Chloro-2-phenylethyl)-4-hydroxy-1*H*-pyrazolo[3,4-*b*]pyridine-5-carboxylic Acid (10). To a solution of 4-chloro-1-(2-chloro-2-phenylethyl)-*1H*-pyrazolo[3,4-*b*]pyridine-5-carboxylic acid ethyl ester **9** (5 g, 13.7 mmol) in 96% ethanol (50 mL) was added 3 M H$_2$SO$_4$ (20 mL). The solution was refluxed 24 h, and the crude precipitate was filtered and recrystallized from absolute ethanol, to give **10** (3.26 g, 75%) as a white solid; mp 228–229 °C. ^{1}H NMR: δ 4.79–4.97 and 5.11–5.29 (2 m, 2H, CH$_2$N), 5.58–5.74 (m, 1H, CHCl), 7.22–7.78 (m, 5H Ar), 8.32 (s, 1H, H-3), 8.76 (s, 1H, H-6). IR cm^{-1}: 3100–2700 (OH), 1641 (CO). Anal. (C$_{15}$H$_{12}$N$_3$O$_3$Cl) C, H, N.

Method A. Example. Methyl 1-(2-Chloro-2-phenylethyl)-4-hydroxy-1*H*-pyrazolo[3,4-*b*]pyridine-5-carboxylate (11a). To a suspension of **10** (1.59 g, 5 mmol) in CH$_3$OH (30 mL) was added 98% H$_2$SO$_4$ (4 mL) dropwise. The mixture was refluxed for 18 h, then concentrated under reduced pressure. The crude was dissolved in CHCl$_3$ (50 mL), washed with a 5% NaHCO$_3$ solution (2 × 20 mL), then with water (20 mL), dried (MgSO$_4$), and evaporated under reduced pressure. The residue was crystallized from absolute ethanol to give **11a** (1.2 g, 72%) as a white solid; mp 138–139 °C. ^{1}H NMR: δ 4.01 (s, 3H, CH$_3$), 4.80–4.95 and 5.01–5.18 (2 dd, 2H, CH$_2$N), 5.51–5.65 (m, 1H, CHCl), 7.28–7.53 (m, 5H Ar), 8.16 (s, 1H, H-3), 8.85 (s, 1H, H-6). IR cm^{-1}: 3100 (OH), 1674 (CO). Anal. (C$_{16}$H$_{14}$N$_3$O$_3$Cl) C, H, N.

Method B. Example. Methyl 4-Chloro-1-(2-chloro-2-phenylethyl)-1*H*-pyrazolo[3,4-*b*]pyridine-5-carboxylate (12a). The Vilsmeier complex, previously prepared from POCl$_3$ (6.13 g, 40 mmol) and anhydrous dimethylformamide (DMF) (2.92 g, 40 mmol), was added to a suspension of **11a** (3.31 g, 10 mmol) in CHCl$_3$ (20 mL). The mixture was refluxed for 8 h. The solution was washed with H$_2$O (2 × 20 mL), dried (MgSO$_4$), and evaporated under reduced pressure, and the residue oil was crystallized by adding absolute ethanol (10 mL) to give **12a** (2.38 g, 68%) as a white solid; mp 113–114 °C. ^{1}H NMR: δ 4.00 (s, 3H, CH$_3$), 4.85–4.97 and 5.06–5.20 (2 dd, 2H, CH$_2$N), 5.53–5.64 (m, 1H, CHCl), 7.26–7.52 (m, 5H Ar), 8.23 (s, 1H, H-3), 9.03 (s, 1H, H-6). IR cm^{-1}: 1729 (CO). Anal. (C$_{16}$H$_{13}$N$_3$O$_2$Cl$_2$) C, H, N.

Cyclopropylmethyl 1-(2-Chloro-2-phenylethyl)-4-hydroxy-1*H*-pyrazolo[3,4-*b*]pyridine-5-carboxylate (13). To a suspension of **10** (0.5 g, 1.57 mmol) in CHCl$_3$ (10 mL) was added thionyl chloride (1.5 g, 12.6 mmol). The mixture was refluxed for 4 h, then concentrated under reduced pressure. To the oil were added CHCl$_3$ (10 mL) and cyclopropylmethanol (2.86 g, 40 mmol), and the solution was refluxed for 6 h. The mixture was then concentrated under reduced pressure, to give a crude oil, that was dissolved in CHCl$_3$ (10 mL) and washed with a 5% NaHCO$_3$ solution (2 × 5 mL) and with water (10 mL). The organic solution was dried (MgSO$_4$), filtered, and evaporated under reduced pressure, and the residue oil was crystallized by adding a mixture 1:1 of diethylic ether/petroleum ether (bp 40–60°C), to give **13** (0.29 g, 50%) as a white solid; mp 101–102°C. ^{1}H NMR: δ 0.35–0.50 and 0.61–0.78 (2m, 4H, 2CH$_2$ cycloprop), 1.20–1.40 (m, 1H, CH cyclo-prop), 4.26 (d, *J* = 7.2, 2H, CH$_2$O), 4.76–4.83 and 5.05–5.20 (2m, 2H, CH$_2$N), 5.52–5.68 (m, 1H, CHCl), 7.22–7.59 (m, 5H Ar), 8.19 (s, 1H, H-3), 8.94 (s, 1H, H-6), 12.20–12.30 (br s, 1H, OH, disappears with D$_2$O). IR cm^{-1}: 3200–3000 (OH), 1671 (CO). Anal. (C$_{19}$H$_{18}$N$_3$O$_3$Cl) C, H, N.

Method C. Example. Methyl 1-(2-chloro-2-phenylethyl)-4-{[2-(4-methoxyphenyl)ethyl]amino} -1*H*-pyrazolo[3,4-*b*]pyridine-5-carboxylate (2h). To a solution of **12a** (0.35 g, 1 mmol) in anhydrous toluene (5 mL) was added 4-methoxyphenethylamine (0.6 g, 4 mmol), and the reaction mixture was stirred at room temperature for 48 h. The mixture was washed with H$_2$O (2 × 10 mL), the organic phase was dried (MgSO$_4$), filtered, and evaporated under reduced pressure, and the residue oil was crystallized by adding petroleum ether (bp 40–60 °C) (5 mL), to give **2h** (0.32 g, 70%) as a white solid; mp 102–103°C. ^{1}H NMR: δ 3.06 (t, *J* = 7.8, 2H, CH$_2$Ar), 3.83 (s, 3H, OCH$_3$), 3.85–3.96 (m, 5H, OCH$_3$+ CH$_2$NH), 4.72–4.87 and 4.97–5.12 (2m, 2H, CH$_2$N), 5.54–5.66 (m, 1H, CHCl), 6.85–7.54 (m, 9H Ar), 8.09 (s, 1H, H-3), 8.84 (s, 1H, H-6), 9.25 (br s, 1H, NH, disappears with D$_2$O). IR cm^{-1}: 3268 (NH), 1680 (CO). Anal. (C$_{25}$H$_{25}$N$_4$O$_3$Cl) C, H, N.

Biological Methods. [^{3}H]DPCPX, [^{3}H]CGS21680 and [^{125}I]-AB-MECA were obtained from DuPont-NEN (Boston, MA). Adenosine deaminase was from Sigma Chemical Co. (St. Louis, MO). All other reagents were from standard commercial sources and of the highest commercially available grade.

A₁ and A₂ₐAR Binding Assay. Affinity of the new compounds toward A₁ and A₂ₐAR was evaluated by competition experiments assessing their ability to displace [^{3}H]DPCPX and [^{3}H]CGS21680 binding from bovine cortical and striatal membranes, respectively. Binding assays were carried out as previously described.[31,32] Pharmacological profile of the most active compounds toward A₁ AR were evaluated by GTP shift assay.[19] Moreover, affinity of the most A₁AR selective compounds was also evaluated in human A₁AR CHO transfected cells (kindly supplied by K. N. Klotz from Wurzburg University, Germany).[33]

A₃AR Binding Assay. [^{125}I]AB-MECA binding to A₃AR in bovine cortical membranes was performed in 50 mM Tris, 10 mM MgCl$_2$, and 1 mM EDTA buffer (pH 7.4) containing 0.2 mg of proteins, 2 U/mL adenosine deaminase, and 20 nM DPCPX. Incubations were carried out in duplicate for 90 min at 25 °C. Nonspecific binding was determined in the presence of 50 μM *R*-PIA and represented approximately 30% of the total binding. The binding reaction was terminated by filtration through a Whatman GF/C filter, washing three times with 5 mL of ice-cold buffer. All compounds were routinely dissolved in dimethyl sulfoxide (DMSO) and diluted with assay buffer to the final concentration (the amount of DMSO never exceeded 2%). At least six different concentrations spanning 3 orders of magnitude, adjusted appropriately for the IC$_{50}$ of each compound, were used. IC$_{50}$ values, computer-generated using a nonlinear regression formula on a computer program (Graph-Pad, San Diego, CA), were converted to K_i values, knowing the K_d values of radioligands in the different tissues and using the Cheng and Prusoff equation.[34]

Computational Chemistry. All calculations were carried out on SGI workstations and a SGI Origin300 server. Due to the fact that biological evaluation of all the new chiral compounds reported here was carried out using racemic mixtures, it was arbitrarily decided to model them with undefined chirality by means of the software Catalyst, thus allowing the software, during the alignment procedure, to choose which configuration of the asymmetric carbon atom common to compounds **1−8** and **77−80** was most appropriate. This decision can be justified on the basis of the fact that a number of chiral compounds was included in the training set and **2h** was used as one of the four template structure. The *S*-**2h** enantiomer has been chosen by the program to be aligned to compound **23** (see below). However, to the best of our knowledge and our results, there are no experimental data supporting the hypothesis that *S* enantiomers are more active than *R* enantiomers in the series of pyrazolo[3,4-*b*]pyridines bearing a 2-chloro-2-phenylethyl side chain at N1.

Catalyst 4.9 was used either to sketch structures with undefined chirality and to perform a conformational search. The best searching procedure was applied to select representative conformers within 5 kcal/mol from the global minimum.

Cerius2 software was applied to align molecules, by application of the Field Fit alignment method (using CFF force field). In detail, Target Model was used as the Align Strategy, Field as the Align Method, and Rigid as the Align Type. A high activity and structural rigidity were the parameters applied to choose the Target Model.

The descriptive steric, electrostatic, and hydrogen bond interactions, represented by the Lennard−Jones energy, the Coulombic energy, and a hydrogen bonding term, respectively, were calculated using GRID, version 21. Analysis was per-

formed using a grid spacing of 1 Å. The grid dimensions were (Å): X_{min}/X_{max}, $-13.0/15.0$; Y_{min}/Y_{max}, $-13.0/13.0$; Z_{min}/Z_{max}, $-11.0/12.0$.

PLS models were calculated using GOLPE, version 4.5.12. The software automatically rejects variables having a total sum of square (SS) less than 10^{-7}. Afterward, an advanced pretreatment was performed that omitted from the analysis grid points (variables) with too low standard deviation values (<0.02). Variables which exhibited only two values were also removed.

Since groups of variables may represent the same structural information as a single variable, after application of the D optimal design criterion, the variables were grouped together according to the Smart Region Definition (SRD) grouping algorithm, selecting a number of 1879 seeds in the PLS weight space with a critical cutoff distance of 1.0 Å and a collapsing cutoff distance of 2.0 Å.

The obtained groups of variables (667 regions) were used in the Fractional Factorial Design (FFD) variable selection procedure, replacing the original variables. Following this protocol, groups of variables instead of single variables were removed from the data file. To evaluate the effect of the grouped variables on the predictivity, a number of reduced models was built by removing the variables according to the FFD design and using 20% of dummies, on the basis of the random group cross-validation approach. In detail, the ligands were randomly assigned to five groups, each one containing an equal number of ligands. Models were built keeping one of these groups out of the analysis (the leave-one-out cross-validation methodology) until all the ligands had been kept out once. The formation of the groups and the validation was repeated 20 times, using a maximum dimensionality of five principal components. After application of the FFD variable selection, 1247 active variables were kept.

Supporting Information Available: Details of the synthesis of compounds **2**–**14** and their elemental analysis data. This material is available free of charge via the Internet at http://pubs.acs.org.

References

(1) Jacobson, K. A.; van Galen, P. J.; Williams, M. Adenosine receptors: pharmacology, structure–activity relationships, and therapeutic potential. *J. Med. Chem.* **1992**, *35*, 407–422.
(2) Daly, J. W. Adenosine receptors: targets for future drugs. *J. Med. Chem.* **1982**, *25*, 197–207.
(3) Collis, M. G.; Hourani, S. M. Adenosine receptor subtypes. *Trends Pharmacol. Sci.* **1993**, *14*, 360–363.
(4) Ralevic, V.; Burnstock, G. Receptors for purines and pyrimidines. *Pharmacol. Rev.* **1998**, *50*, 413–492.
(5) Poulsen, S. A.; Quinn, R. J. Adenosine receptors: new opportunities for future drugs. *Bioorg. Med. Chem.* **1998**, *6*, 619–641.
(6) Müller, C. E.; Scior, T. Adenosine receptors and their modulators. *Pharm. Acta Helv.* **1993**, *68*, 77–111.
(7) Müller, C. E.; Stein, B. Adenosine receptor antagonists: structures and potential therapeutic applications. *Curr. Pharm. Des.* **1996**, *2*, 501–530.
(8) Dhalla, A. K.; Shryock, J. C.; Shreeniwas, R.; Belardinelli, L. Pharmacology and therapeutic applications of A₁ adenosine receptor ligands. *Curr. Top. Med. Chem.* **2003**, *3*, 369–385.
(9) Ribeiro, J. A.; Sebastião, A. M.; de Mendonça, A. Adenosine receptors in the nervous system: pathophysiological implications. *Prog. Neurobiol.* **2002**, *68*, 377–392.
(10) Müller, C. E. A₁ adenosine receptors and their ligands: overview and recent developments. *Farmaco* **2001**, *56*, 77–80.
(11) Chebib, M.; McKeveney, D.; Quinn, R. J. 1-Phenylpyrazolo[3,4-*d*]pyrimidines; structure-activity relationships for C6 substituents at A₁ and A₂A adenosine receptors. *Bioorg. Med. Chem.* **2000**, *8*, 2581–2590.
(12) Terai, T.; Kusonoki, T.; Kita, Y.; Akahane, A.; Shiokawa, Y.; Kohno, Y.; Horiai, H.; Uehara, Y.; Yoshida, K. FK453: A novel nonxanthine adenosine A₁ receptor antagonist as diuretic. *Cardiovasc. Drug Rev.* **1997**, *115*, 44–58.
(13) Daly, J. W.; Hong, O.; Padgett, W. L.; Shamim, M. T.; Jacobson, K. A.; Ukena, D. Non-xanthine heterocycles: activity as antagonists of A₁- and A₂-adenosine receptors. *Biochem. Pharmacol.* **1988**, *37*, 655–664.
(14) Daly, J. W.; Hutchinson, K. D.; Secunda, S. I.; Shy, D.; Padgett, W. L.; Shamin, M. T. 1-Methyl-4-substituted-1*H*-pyrazolo[3,4-*b*]pyridine-5-carboxylic Acid Derivatives: Effect of structural alterations on activity at A₁ and A₂ adenosine receptors. *Med. Chem. Res.* **1994**, *4*, 293–306.
(15) (a) Akane, A.; Kuroda, S.; Itani, H.; Shimizu, Y. Patent NO WO9803507, 1998; *Chem. Abstr.* **1998**, *128*, 154090. (b) Akane, A.; Nishimura, S.; Kuroda, S.; Itani, H. Patent NO JP10182643, 1998; Chem. Abstr. **1998**, *129*, 144876.
(16) Schenone, S.; Bruno, O.; Fossa, P.; Ranise, A.; Menozzi, G.; Mosti, L.; Bondavalli, F.; Martini, C.; Trincavelli, M. L. Synthesis and biological data of 4-amino-1-(2-chloro-2-phenylethyl)-1*H*-pyrazolo[3,4-*b*]pyridine-5-carboxylic acid ethyl esters, a new series of A₁-adenosine receptor (A₁AR) ligands. *Bioorg. Med. Chem. Lett.* **2001**, *11*, 2529–2531.
(17) Bondavalli, F.; Botta, M.; Bruno, O.; Ciacci, A.; Corelli, F.; Fossa, P.; Lucacchini, A.; Manetti, F.; Martini, C.; Menozzi, G.; Mosti, L.; Ranise, A.; Schenone, S.; Tafi, A.; Trincavelli, M. L. Synthesis, molecular modeling studies, and pharmacological activity of selective A₁ receptor antagonists. *J. Med. Chem.* **2002**, *45*, 4875–4887.
(18) Schenone, S.; Bruno, O.; Bondavalli, F.; Ranise, A.; Mosti, L.; Menozzi, G.; Fossa, P.; Manetti, F.; Morbidelli, L.; Trincavelli, L.; Martini, C.; Lucacchini, A. Synthesis of 1-(2-chloro-2-phenylethyl)-6-methylthio-1*H*-pyrazolo[3,4-*d*]pyrimidines 4-amino substituted and their biological evaluation. *Eur. J. Med. Chem.* **2004**, *39*, 153–160.
(19) Da Settimo, F.; Primofiore, G.; Taliani, S.; Marini, A. M.; La Motta, C.; Novellino, E.; Greco, G.; Lavecchia, A.; Trincavelli, L.; Martini, C. 3-Aryl[1,2,4]triazino[4,3-*a*]benzimidazol-4(10*H*)-ones: a new class of selective A₁ adenosine receptor antagonists. *J. Med. Chem.* **2001**, *44*, 316–327.
(20) 4-Amino-1-(2-chloro-2-phenylethyl)-1*H*-pyrazolo[3,4-*b*]pyridine-5-carboxylic acid ethyl ester derivatives as reported in ref 16 (**1a**–**1f**) and 1-(2-chloro-2-phenylethyl)-6-methylthio-1*H*-pyrazolo[3,4-*d*]pyrimidines-4-amino substituted as reported in ref 18 (**77**–**80**).
(21) 1,8-Naphthyridine as reported in ref 30 (**15**–**44**); 1,2,4-triazolo-[4,3-*a*]quinoxalin-1-ones as reported in ref 31 (**45**–**60**); 3-aryl-[1,2,4]triazino[4,3-*a*]benzimidazol-4(10*H*)-ones as reported in ref 19 (**61**–**76**).
(22) When a K_i value is impossible to be determined for a compound, there are two alternative ways for reporting its activity. The first one is to show the percentage of inhibition of specific radioligand binding at the maximum dose of the compound tested (10 μM). Alternatively, for compounds **2d**, **6d**, and **6e**, a $K_i > 10$ μM couldbe reported, similarly to that described for compounds **37** and **38** (ref 30). However, both cases describe inactive compounds. As a consequence, on the basis of the fact that also inactive compounds could be a source of important structural information for qualitative and quantitative structure–activity relashionship analysis, we (*i*. Corelli, F.; Manetti, F.; Tafi, A.; Campiani, G.; Nacci, V.; Botta, M. Diltiazem-like calcium entry blockers: a hypothesis of the receptor-binding site based on a comparative molecular field analysis model. *J. Med. Chem.* **1997**, *40*, 125–131; *ii*.) Tafi, A.; Anastassopoulou, J.; Theophanides, T.; Botta, M.; Corelli, F.; Massa, S.; Artico, M.; Costi, R.; Di Santo, R.; Ragno, R. Molecular modeling of azole antifungal agents active against *Candida albicans*. 1. A comparative molecular field analysis study. *J. Med. Chem.* **1996**, *39*, 1227–1235) and others (*i*. Ragno, R.; Artico, M.; De Martino, G.; La Regina, G.; Coluccia, A.; Di Pasquali, A.; Silvestri, R. Docking and 3-D QSAR studies on indolyl aryl sulfones. Binding mode exploration at the HIV-1 reverse transcriptase nonnucleoside binding site and design of highly active *N*-(2-hydroxyethyl)-carboxamide and *N*-(2-hydroxyethyl)carbohydrazide derivatives. *J. Med. Chem.* **2005**, *48*, 213–223; *ii*. Pauwels, R.; Andries, K.; Debyser, Z.; Kukla, M. J.; Schols, D.; Breslin, H. J.; Woestenborghs, R.; Desmyter, J.; Janssen, M. A. C.; De Clercq, D.; Janssen, P. A. J. New tetrahydroimidazo[4,5,1-*jk*][1,4]-benzodi-azepin-2(1*H*)-one and -thione derivatives are potent inhibitors of human immunodeficiency virus type 1 replication and are synergistic with 2′,3′-dideoxynucleoside analogues. *Antimicrob. Agents Chemother.* **1994**, *38*, 2863–2870) usually chosed to not

omit them from a statistical treatment such as a QSAR study, and assumed that their activity could be approximated to that of the least active compound or to the maximum concentration of the ligand used to perform biological tests. Accordingly, a K_i > 10000 nM (a $-\log K_i = 5.0$) was chosen for compounds **2d**, **6d**, **6e**, **37** and **38**, very similar to that of the least active compound **2e** ($-\log K_i = 5.4$) and to that of the structurally related compund **80** ($-\log K_i = 5.0$), and also corresponding to the maximum concentration of each ligand tested (10 μM).

(23) Nielsen, E. O.; Audouze, K.; Peters, D. New series of morpholine and 1,4-oxazepane derivatives as dopamine D4 receptor ligands: synthesis and 3D-QSAR model. *J. Med. Chem.* **2004**, *47*, 3089−3104.

(24) GOLPE 4.5.12; Multivariate Infometric Analyses: Viale dei Castagni, 16 Perugia, Italy, 1999.

(25) GRID 21; Molecular Discovery Ltd, 215 Marsh Road, Pinner, Middlesex, UK.

(26) Catalyst 4.9, Accelrys, Inc., San Diego, CA, 2003.

(27) Marshall G. R., Barry, C. D.; Bosshard, H. E.; Dammkoehler, R. A.; Dunn, D. A. The conformational parameter in drug design: the active analog approach. In *Computer-Assisted Drug Design*, Olson, E. C., Christoffersen, R. E., Eds.; American Chemical Society: Washington, DC, 1979; Vol. 112, pp 205−226.

(28) Cerius², Version 4.8; Accelrys Inc., San Diego, CA, 2003.

(29) An additional model was also generated by application of the same computational protocol and including DPCPX in the training set. Both statistical parameters ($q^2 = 0.7$ on the training set in a PLS model with five components and a SDEP = 0.57 on the test set) and PLS pseudo-coefficient contour maps were very similar to those of the original 3D QSAR model, suggesting that CPCPX did not bias significantly the generation of the model.

Affinity of DPCPX (expressed as $-\log K_i$) was estimated to be 9.6, in good agreement with the experimental value of 10.2. Alignment of such a compound in the current pharmacophoric model (Figure 2) shows HY1-3 filled by the propyl chain at positions 1 and 3 and by the cyclopentyl ring, respectively. Moreover, the 6- and 2-carbonyl groups are HBA1 and HBA2, respectively, while HBD is the 1-NH group.

(30) Ferrarini, P. L.; Betti, L.; Cavallini, T.; Gianaccini, G.; Lucacchini, A.; Manera, C.; Martinelli, A.; Ortore, G.; Saccomanni, G.; Tuccinardi, T. Study on affinity profile toward native human and bovine adenosine receptors of a series of 1,8-naphthyridine derivatives. *J. Med. Chem.* **2004**, *47*, 3019−3031.

(31) Colotta, V.; Catarzi, D.; Varano, F.; Cecchi, L.; Filacchioni, G.; Martini, C.; Trincavelli, L.; Lucacchini, A. Synthesis and structure−activity relationships of a new set of 2-arylpyrazolo[3,4-c]quinoline derivatives as adenosine receptor antagonists. *J. Med. Chem.* **2000**, *43*, 3118−3124.

(32) Pirovano, I. M.; IJzerman, A. P.; van Galen, P. J. M.; Soudijn, W. The influence of molecular structure of N6-(aminoalkyl)-adenosines on adenosine receptor affinity and intrinsic activity. *Eur. J. Pharmacol*. **1989**, *172*, 185−193.

(33) Catarzi, D.; Colotta, V.; Varano, F.; Calabri, F. R.; Lenzi, O.; Filacchioni, G.; Trincavelli, M. L.; Martini, C.; Tralli, A.; Montopoli, C.; Moro, S. 2-Aryl-8-chloro-1,2,4-triazolo[1,5-*a*]quinoxalin-4-amines as highly potent A1 and A3 adenosine receptor antagonists. *Bioorg. Med. Chem.* **2005**, *13*, 705−15.

(34) Cheng, Y. C.; Prusoff, W. H. Relation between the inhibition constant K_i and the concentration of inhibitor which causes fifty percent inhibition (IC₅₀) of an enzyme reaction. *Biochem. Pharmacol*. **1973**, *22*, 3099−3108.